



Title	Structural studies of amorphous Se under pressure
Author(s)	Tanaka, Keiji
Citation	PHYSICAL REVIEW B, 42, 11245-11251 https://doi.org/10.1103/PhysRevB.42.11245
Issue Date	1990
Doc URL	http://hdl.handle.net/2115/5824
Rights	Copyright © 1990 American Physical Society
Type	article
File Information	PRB42-17.pdf



[Instructions for use](#)

Structural studies of amorphous Se under pressure

Keiji Tanaka

Department of Applied Physics, Faculty of Engineering, Hokkaido University, Sapporo 060, Japan

(Received 11 May 1990)

X-ray-diffraction patterns, macroscopic compressibility, and crystallization in amorphous Se subject to pressure have been investigated. The material exhibits pressure-induced structural modifications in the glassy state and a phase transformation to the hexagonal phase at 120 ± 20 kbar. The observations are discussed on the basis of microscopic and thermodynamic models.

I. INTRODUCTION

How to obtain insight into the structure of amorphous materials is one of the fundamental problems studied extensively for many years. Much work has been carried out using diffraction, extended x-ray-absorption fine structure (EXAFS), Raman scattering techniques, etc., while explicit disorder structures barely emerge from single experimental methods. Versatile studies seem to be needed to elucidate the amorphous structure. In addition to the structural measurements performed under fixed conditions, the investigations of structural modifications introduced by changes in temperature, pressure, and composition may serve as fruitful ideas or reinforce speculations proposed previously.

Another characteristic inherent to amorphous materials is the quasistability, which appears as the glass transition, the crystallization, and the dependence of properties on preparation methods and treatments. These phenomena have also been studied for a long time, while their nature remains to be considered more deeply.

In the present paper, we will examine the pressure-induced structural change and the crystallization phenomenon in amorphous Se (*a*-Se), one of the elemental amorphous materials, which may be suitable for discussing essential features. Substantial work has been performed for structures of *a*-Se and liquid Se at 1 atm and also for pressure-induced effects in hexagonal Se,¹ whereas structural changes in *a*-Se under pressure have rarely been examined. It is known that pressurized *a*-Se undergoes an amorphous-to-crystalline transformation, while the results summarized by Gupta and Ruoff² and Parthasarathy and Gopal³ remain controversial.

At 1 atm and room temperature, Se has at least six crystalline allotropes and the amorphous form.^{4,5} In all these polymorphs, the atoms are covalently bonded in twofold coordination, forming ring and/or chain molecules. The covalent bond lengths and angles are 2.3–2.4 Å and 101°–106°. The microscopic structure of *a*-Se has been investigated extensively, and the recent studies by Andonov⁶ and Corb, Wei, and Averbach⁷ argue that the main constituent is entangled chain molecules. In this respect, *a*-Se may bear some resemblance to the hexagonal (trigonal) Se, consisting of helical chains, which is the stablest form at 1 atm and room temperature. Liquid Se is assumed to be similar in structure to *a*-Se at tempera-

tures near the melting point.^{1,7–10}

For hexagonal Se subjected to pressure, considerable experimental and theoretical work has been carried out.^{11–14} Hydrostatic compression dramatically decreases the interchain distance, with the intrachain configuration being mostly intact. Parthasarathy and Holzapfel have examined the pressure-induced phase transition in hexagonal Se up to 500 kbar (=50 GPa), demonstrating that the hexagonal phase changes into a monoclinic phase at 140 ± 10 kbar accompanying a discontinuous volume change.¹⁵

II. EXPERIMENT

Glassy Se films with 50-μm thickness were obtained by vacuum evaporation onto room-temperature glass plates. The films were peeled off from the substrates, and were pressurized using the standard diamond-anvil-cell technique.¹⁶ The ethanol-methanol mixture, which was known to be fluid up to 104 kbar, was utilized as a pressure transmitting medium. The generated pressure was calibrated with the peak wavelength of the ruby luminescence¹⁶ with an accuracy of ± 3 kbar.

X-ray-diffraction patterns were obtained using Mo K_α radiation emitted from a Rigaku RU-1000 rotating anode set and a position-sensitive proportional counter in conjunction with a data-processing system. For details, see a recent publication.¹⁷ Macroscopic compression behavior of *a*-Se in the pressure cell was examined by direct measurements of sample dimensions using an optical microscope with an image processing system.¹⁸ This technique is suitable for evaluating gross features of pressure (*P*)-length(*L*) relations up to ~ 100 kbar with an accuracy of $\Delta L/L \simeq \pm 0.5\%$. The pressure dependence of the crystallization temperature was determined by inspecting the texture of *a*-Se loaded in the pressure cell, which was heated at a rate of $\sim 10^\circ\text{C}/\text{min}$ using an electrical heater. The technique was practical in a pressure range lower than ~ 30 kbar, in which the generated pressure could be held constant during the temperature increase. When *a*-Se crystallized, the optically flat surface became coarse grained.

III. RESULTS

Figure 1 shows diffraction patterns of *a*-Se subjected to selected levels of pressure. At 1 atm the pattern is similar

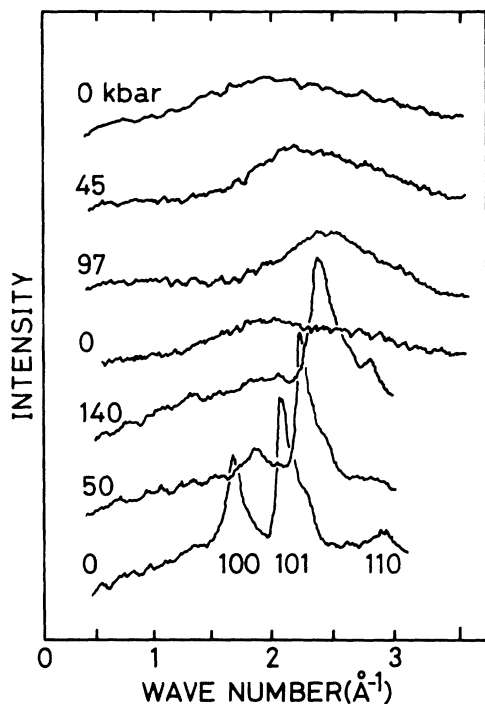


FIG. 1. X-ray-diffraction patterns in *a*-Se under compression. The pressure is changed successively from the upper plot to the lower one. The intensity scale of crystalline samples is reduced to one-half of the amorphous scale. Peak indices in the hexagonal representation are given for the bottom pattern.

to that reported previously;⁶ only a broad halo, the peak being located at 2 \AA^{-1} , is observed in the investigated $Q(=4\pi \sin\theta/\lambda)$ region up to 3.5 \AA^{-1} . With increasing pressure, the halo gradually shifts to higher wave numbers with an increase in the peak height and a decrease in the width. These changes are comparable with those in liquid Se under pressure.⁸ If the sample is released from pressures less than 100 kbar, a pattern almost the same as the initial one is obtained at 1 atm. Hysteresis effects exist in depressurizing processes.¹⁸ However, the sample released to 1 atm seems to be rapidly annealed, since the glass-transition temperature of *a*-Se is just above room temperature (310 K).^{4,6}

If we compress the sample higher than 100 kbar, it is transformed to the hexagonal phase. The precise transition pressure could not be determined in the present experiment. It was between 97 and 140 kbar and microscope observations showed that it was abrupt.¹⁹ Once the structure had been transformed into the crystalline state, the position and the intensity of diffraction peaks changed in a reversible way with pressure, the characteristic which was in agreement with the behaviors reported for the hexagonal Se.^{11,13,15}

The present observations for the amorphous-to-crystalline transformation appear to be in conflict with some previous results in two respects. X-ray studies have been reported only by McCann and Cartz,¹¹ who found that the transformation from amorphous to crystalline states occurs gradually at pressures above 60 kbar. They

have noticed further that the transformed state is an unknown crystal differing from the hexagonal form. The transformation into unresolved metallic structures has been implied by other workers on the basis of electrical measurements.^{2,3} However, we note that most of the early experiments are carried out employing Bridgman anvils, which generate strongly nonhydrostatic stresses.²⁰ The gradual transformation may also be due to nonhydrostatic pressure distribution, since McCann and Cartz¹¹ utilize NaCl as a pressure transmitting material and shear forces are known to decrease the transformation pressure.^{21,22}

Figure 2 shows the pressure dependence of the atomic volume in *a*-Se up to 102 kbar. The result was calculated from the pressure (*P*)-volume(*V*) relation, which was obtained from the experimental *P*-*L* relation under an assumption of isotropic contraction and the density at 1 atm, 4.27 g/cm^3 .²³ The volume change can be fitted to the Murnaghan equation

$$P = (B_0/B')[(V_0/V)^{B'} - 1], \quad (1)$$

where B_0 and B' represent the bulk modulus and its pressure derivative, and the subscript 0 means the value at $P=0$. A least-squares-fitting procedure gives $B_0=94$ kbar and $B'=5$. These results may be compared with previous data,^{3,24} $B=67.8\text{--}92.9$ kbar and $B'=3.2\text{--}8.5$ kbar, which have been obtained in pressure regions lower than 50 kbar. In Fig. 2, the result for hexagonal Se, which is calculated from x-ray-diffraction data (the density at 1 atm, 4.82 g/cm^3),^{13,15} is also plotted for comparison.

Figure 3 shows the pressure dependence of the crystallization temperature T_c , together with the dependences of the melting temperature T_m ,⁸ and the glass-transition temperature T_g .^{25,26} As is well known, the

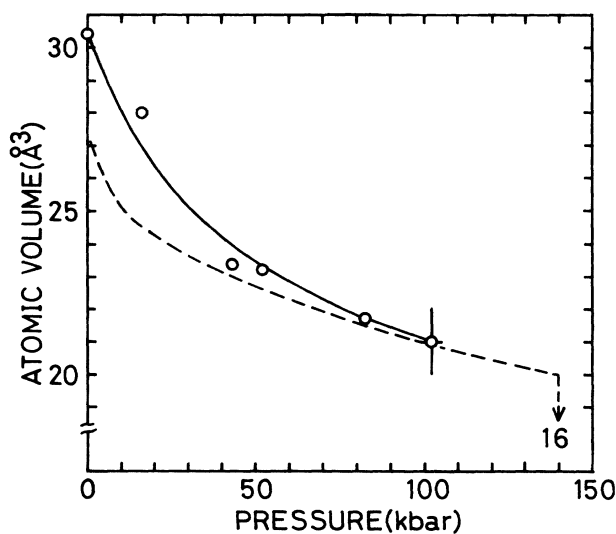


FIG. 2. Pressure dependences of the atomic volume in *a*-Se (open circles with solid line) and hexagonal Se (dashed line). The error bars attached to the 103-kbar point apply to other experimental points. The hexagonal form undergoes a phase transition to a monoclinic form with an atomic volume of 16 \AA^3 at 140 kbar.

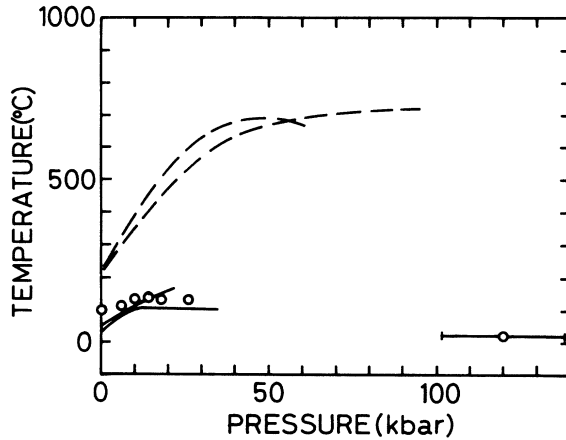


FIG. 3. The pressure dependence of the melting temperature T_m (dashed line), the crystallization temperature T_c (open circles), and the glass-transition temperature T_g (solid line). An error bar is attached for the T_c datum at 120 kbar. For references of T_m and T_g , see the text.

crystallization and glass-transition temperatures may vary about $\pm 10^\circ\text{C}$, depending upon experimental conditions such as heating rate, and thus we remark upon only the gross features. In a low-pressure region, the crystallization temperature appears to change nearly in parallel with the glass-transition temperature, but the crystallization induced by compression of 120 kbar at room temperature seems to occur below the glass-transition temperature.

IV. DISCUSSION

In the following, we will examine two problems: (i) the structure and its change in a -Se under compression and (ii) why the pressure-induced transformation from the amorphous to the hexagonal phase occurs at room temperature.

Several structural models have been proposed to interpret physical properties in a -Se,^{1,6,7,27} and in order to discuss an essential feature of the pressure-induced structural change we adopt a microcrystalline model illustrated in Fig. 4. That is, we assume tentatively that the local

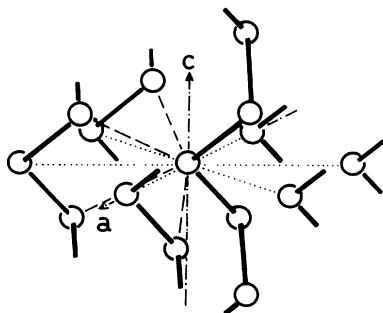


FIG. 4. A local structure of hexagonal Se. R_1 and R_2 pairs (Table I) with the central atom are connected by dashed and dotted lines, and a and c crystalline axes are indicated.

structure of a -Se resembles the hexagonal Se structure, with three reasons: (i) almost all structural and electronic data indicate that the main constituent of a -Se is the chain molecule, though ring molecules may be contained in the minority,⁷ (ii) consideration of the intermolecular distance is necessary to interpret the present result, and for this purpose the hexagonal structure is adequate, and (iii) substantial pressure data are reported for the crystalline form. The relevant structure parameters of hexagonal Se at 1 atm and 100 kbar are listed in Table I.¹³

The microcrystalline model is consistent with the x-ray patterns. Figure 1 implies that the halo at $\sim 2 \text{ \AA}^{-1}$ can be regarded as a convolution of 100, 101, and 110 hexagonal peaks.²⁸ The pressure-induced changes in the amorphous halo and the crystalline peaks bear a remarkable resemblance to each other in intensity and position. The overall feature of the halo patterns can be reproduced by convolution of these peaks which are broadened as Gaussian functions. The crystalline size t estimated from the reproduction using the Scherrer equation, which is applicable to chain molecules,²⁹

$$t = \lambda / (B \cos \theta_B), \quad (2)$$

is about 20 \AA . Here λ is the x-ray wavelength, B is the full width at half maximum, and θ_B is the Bragg angle. Similar magnitudes are inferred from radial-distribution-function (RDF) analyses for a -Se at 1 atm.⁷ This scale, which is greater than the unit-cell dimension of hexagonal Se (Table I), may provide justification for adapting the microhexagonal structure as a guiding model of a -Se.

To get insight into the amorphous structure, we may follow the Debye scattering equation for the diffracted x-ray intensity $I(Q)$:

$$I(Q) = \sum_{m,n} f_m f_n \sin(Qr_{mn}) / (Qr_{mn}), \quad (3)$$

where f is the atomic scattering factor and r is the separation between a pair of atoms identified by the subscripts m and n . Since the scattering factor undergoes a smooth modification with the scattering angle and the present patterns shown in Fig. 1 are limited to a small Q region, f

TABLE I. Atomic distances, unit-cell dimensions (in units of \AA), atomic volumes at 1 atm and 100 kbar, and the coordination number Z in hexagonal Se. Note that R_2 is equal to the (100) plane distance.

	1 atm	100 kbar	Z
First-nearest intrachain bond length, r_1	2.38	2.40	2
Second-nearest intrachain bond length, r_2	3.71	3.81	2
First-nearest interchain distance, R_1	3.44	2.97	4
Second-nearest interchain distance, R_2	4.37	3.75	6
Unit-cell dimension a	4.37	3.75	
Unit-cell dimension c	4.96	5.12	
Atomic volume (\AA^3)	81.9	62.2	

can be assumed to be a constant. Then, Eq. (3) predicts that the atomic pairs separated at r give the most intense peak at $Q_1 = 7.72/r$. Thus, we may argue that the halo extending $1.5\text{--}2.5 \text{ \AA}^{-1}$ at 1 atm is a convolution of the pairs separated at r_2 , R_1 , and R_2 listed in Table I.

Figure 5 shows the calculated patterns at 1 atm and 100 kbar using the expression

$$I(Q) = \sum_i Z(r_i) \sin(Qr_i) / (Qr_i), \quad (4)$$

where Z is the coordination number, and the summation is taken over the r_2 , R_1 , and R_2 pairs, in which the interchain distances are expanded from the crystalline values according to the relation

$$R^a = R^c (v_a^a / v_a^c)^{1/2}, \quad (5)$$

where v_a is the atomic volume, and the superscripts a and c denote amorphous and crystalline. (This notation applies throughout the text.) Note that the power $\frac{1}{2}$ is due to the relation $v_a \propto R^2$, which may be applicable to one-dimensional molecules.^{30,31} For numerical values of concern, the data in Table I and Fig. 2 have been employed.

We see in Fig. 5 that the overall features are in agreement with the x-ray patterns shown in Fig. 1. The halo peak shifts with pressure, and the difference of the peak positions at 1 atm and 100 kbar is 0.35 \AA^{-1} , comparable with the experimental result. This peak shift is caused by a dramatic decrease in the interchain distances, which is known to govern the pressure dependence of electronic properties.^{3,25,32,33} It is emphasized that inclusion of the pairs separated at R_2 is important for the numerical analysis. As is seen from the interference patterns of

each component (Fig. 5), if we neglect the R_2 pairs, the halo becomes broader with pressure since r_2 hardly changes and R_1 decreases substantially. The inclusion contributes to narrowing the width, resulting in a qualitative agreement with the experimental patterns.

However, in the model calculation, the peak positions are located at values of Q that are $0.2\text{--}0.3 \text{ \AA}^{-1}$ lower than the experimental data, and the intensity increasing and the peak narrowing may not be reproduced satisfactorily. A possible way to improve the agreement is to modify the coordination numbers Z for the pairs at R_1 and R_2 . In hexagonal Se, these are 4 and 6. If we increase $Z(R_1)$ and decrease $Z(R_2)$, which may result from disordering the intermolecular configuration, the agreement will become better. Such chain structures may be envisaged, since a -Se is considered to be substantially disordered with respect to the interchain correlation. More refined analyses will need realistic structural models which include the structural randomness and its changes by compression, such as the fracture of covalent bonds and the cross linking between chain molecules.^{9,33}

Regarding the structural change from the amorphous to the hexagonal phase, we first consider the variation of the atomic volume shown in Fig. 2. Although the present result for the volume change in a -Se is limited to pressures of less than 102 kbar, it seems that the phase transformation from the glassy to the hexagonal form, existing at 120 ± 20 kbar (Fig. 1),¹⁹ accompanies no appreciable volume change. The amorphous and crystalline phases may have nearly the same density at the critical pressure. In addition, the atomic volume of the amorphous sample appears to approach asymptotically the crystalline value, i.e., $\Delta k = k^a - k^c = 0$, where k is the compressibility.

The above peculiar feature may be consistent with the pressure dependence of the crystallization temperature T_c shown in Fig. 3. Applying the Ehrenfest equation, which is based on a continuity of volume at a transition, to the amorphous-to-crystalline transformation we obtain

$$dP/dT_c = \Delta\beta / \Delta k, \quad (6)$$

where $\Delta\beta (= \beta^a - \beta^c)$ is the thermal-expansion difference. As mentioned above, $\Delta k \approx 0$ and in contrast $\Delta\beta > 0$ may be retained under pressure.³⁴ Then $dP/dT_c = \infty$, which means that the pressure dependence of T_c is very weak.³⁵ This result appears to be in harmony with the low-pressure data of T_c shown in Fig. 3. The weak dependence implies that the critical pressure of the transformation may change substantially depending upon experimental details; the implication may be partly responsible for the scattered transformation pressures, 60–140 kbar at room temperature.^{2,3}

Crystallization phenomena of amorphous materials under pressure may be treated in two ways. The first is the thermodynamic transition model from an equilibrium to another equilibrium phase.³⁶ Although the amorphous phase is in quasiequilibrium, the concept can be applied to the pressure-induced crystallization of a -Ge to the β -Sn phase, since the β -Sn phase has a higher equilibrium energy than that of the amorphous phase.³⁷ The energy needed for the transition is supplied with compressive

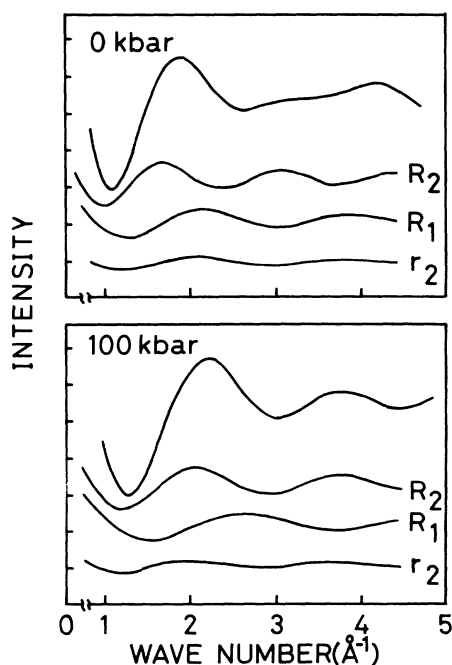


FIG. 5. Calculated diffraction patterns (top curves) and the components (Table I) at 0 and 100 kbar.

forces. The second treatment refers to the crystal growth which occurs in nonequilibrium states such as in supercooled liquids. This phenomenon is a kind of relaxational transformation to lower energy states.³

The crystallization of *a*-Se cannot be understood in light of the thermodynamic phase-transition model, since as shown in Fig. 6 the Gibbs free energy of *a*-Se may be greater than that of the hexagonal phase at pressures of interest.³⁸ This result is obtained as follows. The pressure dependence of the Gibbs free energy *G* is given as

$$G(P) = \int_0^P V(P) dP. \quad (7)$$

Combining this equation with Eq. (1), *G*(*P*) in crystalline Se can be evaluated under a reference *G*(0)=0. The amorphous material is not an equilibrium system and rigorous thermodynamic arguments cannot be applied, whereas its free energy is a useful thermodynamic quantity if the fictive temperature, which may be equated to *T_g* in the present case, is introduced.³⁹ Hence, at 1 atm the difference of the free energies in the amorphous and the crystalline phases may be written as

$$\Delta G = G^a - G^c = H - T_g S_c, \quad (8)$$

where *H* is the enthalpy of crystallization, 47–52 meV,^{4,6} and *S_c* is the configurational entropy 0.43*k_B*,⁴⁰ which give $\Delta G = 40$ meV. The pressure dependence of the entropy term cannot be evaluated at present, and we tentatively neglect it. Then, using Eq. (7), we can estimate *G*(*P*) for the amorphous phase. The accuracy determined by the modulus uncertainty $\Delta B_0 \approx \pm 4$ kbar and $\Delta B' \approx 0.5$ is better than ± 5 meV. However, upon employing Eq. (7), we have assumed implicitly that the *V*(*P*) characteristic for *a*-Se shown in Fig. 2 is elastic, which is not satisfied in the present case.^{18,37} Accordingly, the numerical evaluation is risky, although it may be conceiv-

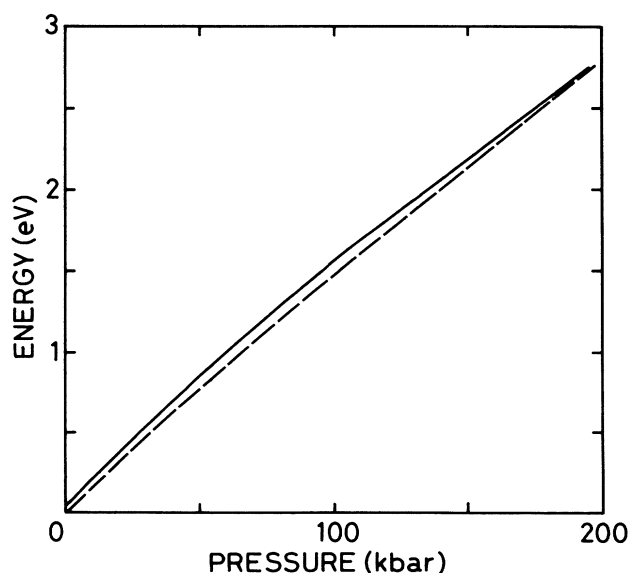


FIG. 6. The pressure dependence of the Gibbs free energies in amorphous (solid line) and hexagonal (dashed line) Se.

able that $\Delta G(P) \geq 0$ at pressures of interest. We therefore follow the crystal-growth model.

It should be pointed out, however, that the observed crystallization temperature seems exceptionally low, and the theoretical treatments known to date may not work out straightforwardly. Most of the crystallization processes in amorphous materials are induced at temperatures between *T_g* and *T_m*. For instance, previous pressure-enhanced crystallization experiments for oxides^{21,41} and chalcogenide⁴² glasses have been carried out at this temperature range, and thus conventional crystal-growth models for supercooled liquids may be applied. Photo- and thermal crystallizations in *a*-Se have been extensively studied, and also become appreciable at temperatures higher than *T_g*.⁴³ In contrast, as shown in Fig. 3, the crystallization at ~ 120 kbar appears to proceed at a temperature below *T_g*, through a direct conversion of the noncrystalline solid into the crystalline state. This fact may imply that in *a*-Se under high pressure, the glass-transition does not occur as in *a*-Te at 1 atm.⁴⁴

The configuration-energy diagram for the crystallization process at 1 atm can be illustrated as shown in Fig. 7. The energy difference between the amorphous and the hexagonal phase may be weakly dependent upon pressure as shown in Fig. 6. In contrast, we can assume that the barrier height, which is about 1 eV at 1 atm,⁴³ decreases dramatically with pressure, and hence the crystallization rate at room temperature is enhanced. The problem is therefore reduced to find the mechanism of the height reduction.

Microscopic structural models have been proposed for the pressure-induced crystallization in Se. It is known that hexagonal Se exhibits a phase transition to a monoclinic structure at 140 ± 10 kbar, which corresponds to $R_1(P)/R_1(0) = 0.85$.¹⁵ In the hexagonal crystal, the intrachain bonding charges are assumed to be transferred to the interchain regions with increasing pressure. Martin, Fjeldly, and Richter have pointed out that the non-bonding *p*-electron orbitals overlap with antibonding states at neighboring chains, which weakens the intrachain bond and strengthens the interchain bond, leading to the hexagonal-to-monoclinic phase transition.¹² The redistribution of the electron charges is demonstrated

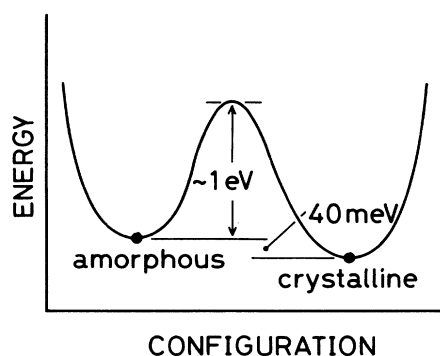


FIG. 7. Configuration diagram of hexagonal and amorphous Se at 1 atm.

theoretically by Starkloff and Joannopoulos.¹⁴ Following this idea, Litov and Anderson²⁴ have assumed that the interchain potential $E(R)$ in α -Se can be approximated as

$$E(R) = A/R^{12} - B/R^6 - C \exp(-\alpha R), \quad (9)$$

where A , B , C , and α are constants. The last term represents the attractive interaction resulting from the charge redistribution. Using some experimental values, and a criterion for the bulk modulus of the phase transition, i.e., $B(P_c) = 0$, they have predicted that the transformation in α -Se occurs when $R_1(P)/R_1(0) = 0.86$. As demonstrated in Fig. 2, however, the transformation occurs when the bulk moduli of amorphous and hexagonal Se are nearly the same.

Although the theoretical treatment by Litov and Anderson²⁴ deviates from the present experimental observations, we may follow the essence of their argument. As shown in the analysis of the x-ray results, the dramatic contraction of the interchain distance is induced by pressurizing. The interchain distance in α -Se must fluctuate spatially reflecting random structures, and then, at some local regions where the interchain distance is shorter than the average, the critical condition $R_1(P)/R_1(0) = 0.86$ may be fulfilled. A bond interchange occurs, which is responsible for crystalline nucleation, and as a consequence, the peripheral parts will successively be converted into the crystalline phase. In this crystal-growth process, no macroscopic atomic diffusion is needed, since the densities of the amorphous and the hexagonal phases are nearly the same as shown in Fig. 2. However, to make this speculation quantitative, we need detailed insight into the degree of the interchain-distance fluctuation as a function of pressure.

The crystallization processes in organic chain molecules have been extensively studied, and accordingly it may be valuable to compare the present speculation with these studies. Crystallization of organic molecules such as polyethylene is considered to proceed through reptant motions of the chain molecules, which form lamellae crystals.⁴⁵ Since α -Se at temperatures above T_g also crystallizes thermally into lamellae structures,⁴⁶ the reptant-motion model may apply to the inorganic chain segments.⁴⁷ In contrast, the crystallization at low temperatures ($T < T_g$) conceivably occurs through the bond interchange as discussed above.

V. SUMMARY

Structure in α -Se under pressure up to 140 kbar has been studied. The pressure-induced change in the x-ray-diffraction patterns can be accounted for using a micro-crystalline model, which assumes a dramatic contraction between the interchain distances. It is suggested that, besides the first-nearest interchain atomic pairs, the second-nearest pairs give an important contribution to the observed change in the diffraction halo at 2 \AA^{-1} .

The disordered phase transforms into the hexagonal crystalline structure at 120 ± 20 kbar without showing appreciable volume and compressibility discontinuities. The crystallization phenomenon is discussed on the basis of thermodynamic and atomic models.

ACKNOWLEDGMENTS

The author would like to thank Dr. Y. Okamoto for fruitful discussions.

¹The Physics of Selenium and Tellurium, edited by E. Gerlach and P. Grosse (Springer-Verlag, Berlin, 1979).

²M. C. Gupta and A. L. Ruoff, J. Appl. Phys. **49**, 5880 (1978).

³G. Parthasarathy and E. S. R. Gopal, Bull. Mater. Sci. **7**, 271 (1985).

⁴Selenium, edited by R. A. Zingaro and W. C. Cooper (Van Nostrand, New York, 1974), Chaps. 1 and 3.

⁵K. Nagata, Y. Miyamoto, H. Nishimura, H. Suzuki, and S. Yamasaki, Jpn. J. Appl. Phys. **24**, L858 (1985).

⁶P. Andonov, J. Non-Cryst. Solids **47**, 297 (1982).

⁷B. W. Corb, W. D. Wei, and B. L. Averbach, J. Non-Cryst. Solids **53**, 29 (1982).

⁸K. Tsuji, O. Shimomura, K. Tamura, and H. Endo, Z. Phys. Chem. Neue Folge **156**, 495 (1988).

⁹K. Tsuji, J. Non-Cryst. Solids **117/118**, 27 (1990).

¹⁰D. Hohl and R. O. Jones, J. Non-Cryst. Solids **117/118**, 922 (1990).

¹¹D. R. McCann and L. Cartz, J. Chem. Phys. **56**, 2552 (1972).

¹²R. M. Martin, T. A. Fjeldly, and W. Richter, Solid State Commun. **18**, 865 (1976).

¹³R. Keller, W. B. Holzapfel, and H. Schulz, Phys. Rev. B **16**, 4404 (1977).

¹⁴Th. Starkloff and J. D. Joannopoulos, J. Chem. Phys. **68**, 579 (1978).

¹⁵G. Parthasarathy and W. B. Holzapfel, Phys. Rev. B **38**, 10 105 (1988).

¹⁶A. Jayaraman, Rev. Sci. Instrum. **57**, 1013 (1986); I. L. Spain, Contemp. Phys. **28**, 523 (1987).

¹⁷K. Tanaka and S. Nitta, Phys. Rev. B **39**, 3258 (1989).

¹⁸K. Tanaka and J. Maeda, Rev. Sci. Instrum. **57**, 500 (1986).

¹⁹The transition pressure 120 ± 20 kbar should be accepted cautiously, since the generated pressure was not hydrostatic above 104 kbar, and anisotropic compression may lower the transition pressure (Refs. 21 and 22). Experiments employing gaseous pressure-transmitting media are desired (Ref. 16).

²⁰C. A. Swenson, in Solid State Physics, edited by F. Seitz and D. Turnbull (Academic, New York, 1960), Vol. 11, p. 41; M. Wakatsuki, K. Ichinose, and T. Aoki, Jpn. J. Appl. Phys. **11**, 578 (1972).

²¹S. Sakka and J. D. Mackenzie, J. Non-Cryst. Solids **1**, 107 (1969).

²²S. B. Quadri, E. F. Skelton, and A. W. Webb, J. Appl. Phys. **54**, 3609 (1983).

²³Since the density was not measured in the present study, we employed an average value reported, $4.25\text{--}4.29 \text{ g/cm}^3$ (Refs. 4–7). The values are not scattered widely, and thus the discussion in Sec. IV is not affected by the density variation.

²⁴E. Litov and O. L. Anderson, Phys. Rev. B **18**, 5705 (1978).

- ²⁵K. Tanaka, Phys. Rev. B **30**, 4549 (1984); Jpn. J. Appl. Phys. **25**, 779 (1986).
- ²⁶A. P. Kuyanov, M. I. Kop'ev, and V. T. Borisov, Dokl. Akad. Nauk SSSR **280**, 866 (1985) [Sov. Phys.—Dokl. **30**, 176 (1985)]; P. J. Ford, G. A. Saunders, E. F. Lambson, and G. Carini, Philos. Mag. Lett. **57**, 201 (1988).
- ²⁷G. Lucovsky and C. K. Wong, Philos. Mag. B **52**, 331 (1985).
- ²⁸The widths of the crystalline peaks are due to the measuring system.
- ²⁹A. M. Hindle and D. J. Johnson, Polymer **21**, 929 (1980).
- ³⁰K. Tanaka, Phys. Rev. B **39**, 1270 (1989).
- ³¹In contrast, when evaluating the bulk compressibility, $v_a \propto R^3$ seems to be a more plausible assumption. See Refs. 24 and 25.
- ³²S. Minomura, in *Amorphous Semiconductors*, edited by Y. Hamakawa (North-Holland, Amsterdam, 1982), p. 245.
- ³³K. Tanaka and H. Murayama, Solid State Commun. **64**, 125 (1987); K. Tanaka, in *Disordered Systems and New Materials*, edited by M. Borisssov, N. Kirov, and A. Vavrek (World Scientific, Singapore, 1989), p. 290.
- ³⁴Yu. I. Krotov, J. Non-Cryst. Solids **105**, 275 (1988).
- ³⁵The same conclusion may be derived from the Clausius-Clapeyron equation, which is based on a continuity of the Gibbs free energy, since the volume change at the transition is negligible.
- ³⁶D. Turnbull, in *Solid State Physics*, edited by F. Seitz and D. Turnbull (Academic, New York, 1956), Vol. 3, p. 225.
- ³⁷K. Tanaka, Solid State Commun. (to be published).
- ³⁸In addition, a common tangent line between the Helmholtz free-energy curves of the amorphous and the hexagonal phases cannot be drawn (see Ref. 37), which is the situation that makes the phase-transition model inapplicable [E. A. Guggenheim, *Thermodynamics* (North-Holland, Amsterdam, 1959)].
- ³⁹A. Q. Tool, J. Am. Ceram. Soc. **29**, 240 (1946); R. S. Hemley, A. P. Jephcoat, H. K. Mao, L. C. Ming, and M. H. Manghani, Nature **334**, 52 (1980).
- ⁴⁰L. Judovits and B. Wunderlich, J. Therm. Anal. **30**, 895 (1985).
- ⁴¹M. J. Aziz, E. Nygren, J. F. Hays, and D. Turnbull, J. Appl. Phys. **56**, 2233 (1985).
- ⁴²M. Shimada and F. Dache, Inorganic Chem. **16**, 2094 (1977); G. Devaud, M. J. Aziz, and D. Turnbull, J. Non-Cryst. Solids **109**, 121 (1989).
- ⁴³J. Dresner and G. B. Stringfellow, J. Phys. Chem. Solids **29**, 303 (1968); D. X. Pang, J. T. Wang, and B. Z. Ding, J. Non-Cryst. Solids **107**, 239 (1989).
- ⁴⁴T. Takahashi and Y. Harada, J. Non-Cryst. Solids **47**, 417 (1982).
- ⁴⁵P. G. DeGennes, *Scaling Concepts in Polymer Physics* (Cornell University Press, Ithaca, 1979), Sec. 8; M. Hikosaka, Polymer **21**, 929 (1987).
- ⁴⁶R. B. Stephens, J. Appl. Phys. **51**, 6197 (1980).
- ⁴⁷It should be mentioned, however, that the intrachain bond strength in Se, ~ 2 eV, is approximately one-tenth of the organic values.